

Research Paper

The Effect of Surface Hardening on The HQ 705 Steel Camshaft Using Static Induction Hardening and Tempering Method

Sri Nugroho¹, Deni Fajar Fitriyana², Rifky Ismail¹, Thesar Aditya Nurcholis¹,
Tezara Cionita³, Januar Parlaungan Siregar⁴

¹Department of Mechanical Engineering, Faculty of Engineering, Diponegoro University, Jl. Prof. Sudarto No.13, Tembalang, Semarang, 50275, Indonesia

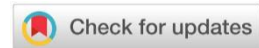
²Department of Mechanical Engineering, Faculty of Engineering, Universitas Negeri Semarang, Kampus Sekaran, Gunungpati, Semarang, 50229, Indonesia

³Department of Mechanical Engineering, Faculty of Engineering and Quantity Surveying, INTI International University, 71800 Nilai, Negeri Sembilan, Malaysia

⁴Department of Mechanical Engineering, College of Engineering, Universiti Malaysia Pahang, 26300 Gambang, Kuantan, Malaysia

srinugroho.undip@gmail.com

<https://doi.org/10.31603/ae.7029>



Published by Automotive Laboratory of Universitas Muhammadiyah Magelang collaboration with Association of Indonesian Vocational Educators (AIVE)

Abstract

Article Info

Submitted:

22/04/2022

Revised:

27/05/2022

Accepted:

31/05/2022

Online first:

11/06/2022

Induction hardening (IH) is a popular choice for automotive components such as camshafts for its ability to harden portions of a component selectively. The camshaft will contact the tappet, connected to the rocker arm, to open and close the valve whenever the engine is running. This contact between the camshaft and the tappet causes wear on the camshaft surface. IH of the camshaft is required to improve wear resistance and service life, as well as core elasticity to absorb high torsional stresses. It is known that studies about IH on camshafts are still very limited. This study aims to determine the effect of the induction hardening and tempering treatment on the mechanical properties of the camshaft made of HQ 705 steel. The induction hardening carried out in this study uses different parameter settings such as heating time and output current. The camshaft specimen is hardened by static induction and then quenched in oil. The specimens are tempered after induction hardening with different temperatures and holding times to adjust the hardness level and reduce brittleness. Hardness, macro photographs, micrograph, and wear tests were conducted to determine the mechanical properties of the camshaft specimen after the induction hardening and tempering process. This study indicates that induction hardening with an output current of 747 A for 15 seconds followed by tempering at 150 °C for 15 seconds on specimen 1 produced the best mechanical properties. On the surface of these specimens found more martensite content while there was no microstructural change on the inside. The surface hardness of these specimens is 44 HRC (Rockwell C Hardness), while the inside is 26 HRC. Meanwhile, specific wear decreased by 45.45%.

Keywords: Surface hardening; Camshaft; Induction; Quenching; Tempering

1. Introduction

The overhead-valve train system in the diesel engine consists of a camshaft, tappet, pushrod, rocker arm, upper retainer, valve spring, fixed retainer, valve guide, valve, and valve seat [1]. The camshaft is used to open and close the intake and exhaust valves of the diesel engine at certain

intervals. They work under high speed, variable load, and complex elasto-hydrodynamic lubrication conditions. The camshaft will be in direct contact with the tappet, connected to the pushrod and rocker arm to open and close the valve when the engine is running. This contact between the camshaft and the tappet causes



This work is licensed under a Creative Commons Attribution-NonCommercial 4.0 International License.

surface scuffing, pitting, and abnormal wear on the camshaft surface. To prevent the occurrence of surface scuffing, pitting, and abnormal wear, the camshaft surface is treated using the induction hardening method to enhance the surface hardness, wear resistance, and service life of the cams, specifically in the area related to cam lobe and journal [2], [3].

Induction hardening is a popular method for surface treatment of a variety of automotive components, including camshafts. Induction hardening is when the heat is generated directly in the workpiece with preheating, heating, quenching, and tempering stages. This method is more economical and environmentally friendly because heat energy is created using electricity without burning fossil fuels. Additionally, induction heating can be precisely controlled via the number and design of coil, specimen diameter, input current, frequency, heating time, and temperature. This minimises deformation in the workpiece and ensures the hardening process's efficiency and hardness depth [4], [5]. The use of the induction hardening method to increase automotive components' hardness and wear resistance has been widely studied. The increased wear resistance of camshaft material made from ductile cast iron with the induction hardening method has been studied by Karaca et al., 2017. The wear resistance of the camshaft increases with increased austenitisation temperature, time, and induction hardening. The best wear resistance of the camshaft has been obtained in a combination of austempering (900 °C, 90 minutes) and the induction hardening process [6].

The increase in temperature and duration during the induction hardening process on gear were made from S45C steel causes a large amount of heating propagation throughout the gear specimen. After quenching, the austenite phase transforms into martensite phase with very hard and brittle properties. This causes the surface hardness of the material to increase, but the distortion is getting more prominent [7].

The surface hardness of the crankshaft material made of 50CrMo4 steel increases with induction hardening. In addition, fatigue strength is

increased by 45% after the induction hardening process [8]. The studies about the induction hardening process on camshafts material made of HQ 705 steel are still very limited. Therefore, this study aims to determine the effect of induction hardening and tempering on surface hardness and wear resistance of the camshaft material made of HQ 705 steel. Induction hardening treatment was carried out using the static method to obtain the minimum hardness required on the camshaft surface without changing the material's inner hardness. The minimum hardness required on the surface of the camshaft is 45 HRC [9]. Furthermore, the parameters used in this study will be evaluated for application on camshafts for rural cars with a 990-cc engine capacity by the Agency for The Assessment and Application of Technology (BPPT), Indonesia.

2. Method

In this study, HQ 705 steel with a cylindrical rod shape was provided by the Agency for the Assessment and Application of Technology (BPPT), Indonesia. The chemical composition of HQ 705 Steel was tested using an Optical Emission Spectroscopy Switzerland QTD-127. **Table 1** shows the chemical composition of the HQ 705 steel used in this study. HQ 705 steel is a high strength low alloy steel which has an excellent combination of toughness, fatigue resistance, and ductility, making it suitable for use in applications requiring very high levels of strength, such as aircraft landing gear, high strength bolts, power transmission gears, shafts, and airframe part [10]–[12].

The wire cutting machine is used to cut the cylindrical rod of HQ 705 steel into a camshaft specimen (cam), as shown in **Figure 1** and **Figure 2**. The annealing heat treatment was carried out at a temperature of 870 °C for 30 minutes using the Thermolyne F6010 furnace and then left to room temperature in the furnace. The annealing process is performed on the camshaft specimen to increase its flexibility and reduce its hardness [13]. The hardness of the camshaft specimen made from HQ 705 before and after the annealing process were 33 HRC and 25 HRC.

Table 1. Chemical composition of HQ 705

Element	C	Si	Mn	P	S	Cr	Mo	Ni
Percentage	0.37	0.4	0.72	< 0.020	< 0.005	1.41	0.22	1.29

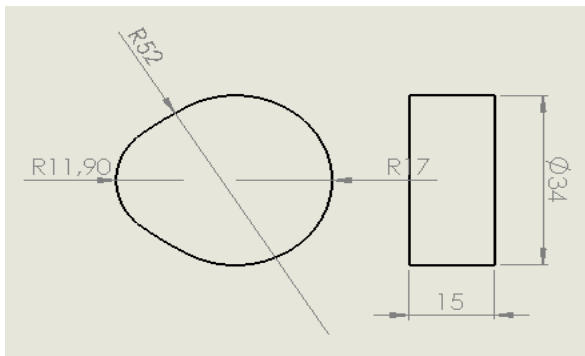


Figure 1. Camshaft dimension design (mm)

In this study, the induction machine single-phase 220V (50/60Hz) is used for induction hardening, where oil was used as a cooling fluid in the quenching process [14]. A handmade coil with 2 turns of wire was prepared to harden the specimen with a 4 mm gap to the outer diameter of the specimen [15]. First, the induction hardening process in specimens 1 and 2 was carried out with an output current of 747 A for 15 and 20 seconds. Then tempering was carried at a temperature of 150 °C for 15 and 20 seconds for specimens 1 and 2. Next, in specimens 3 and 4, induction hardening was performed at an output current of 985 A for 15 and 20 seconds, respectively. During the induction heating, the input current and heating duration are measured with a clamp meter and a stopwatch.

The output current is controlled using the induction machine's display. Finally, the tempering process on specimens 3 and 4 was carried out at a temperature of 250 °C with a

holding time of 15 and 20 seconds, respectively. The level of these parameters is given in **Table 2**.

Tempering was done in this study utilizing induction heating equipment with a 290 A output current. The process of tempering is shown in **Figure 3**. An infrared thermometer and a thermocouple installed on the induction machine were used to measure the temperature of the specimen during the tempering process. The material is left in the open air after achieving the specified temperature and holding time so that the temperature gradually drops to room temperature. In this study, the tempering process is not carried out in specimen 4 because the material melts during induction hardening, as shown in **Figure 4**.

Macrographic, micrographic, and hardness tests were carried out on the specimens after induction hardening and tempering. The macrograph examination is used to obtain a macro photograph of an induction-hardened camshaft specimen indicating the case/surface, core, and transition regions [16], [17]. The macrograph of the camshaft specimens was observed by optical microscopy (OM). A metallographic method is used to examine the microstructure of a camshaft specimen that has been induction hardened and tempered. The sample was prepared from induction hardening, and tempering is mounted, polished, and then etched with a 2% nitric acid solution [18]. The optical microscope (OM) was used to examine the microstructure.

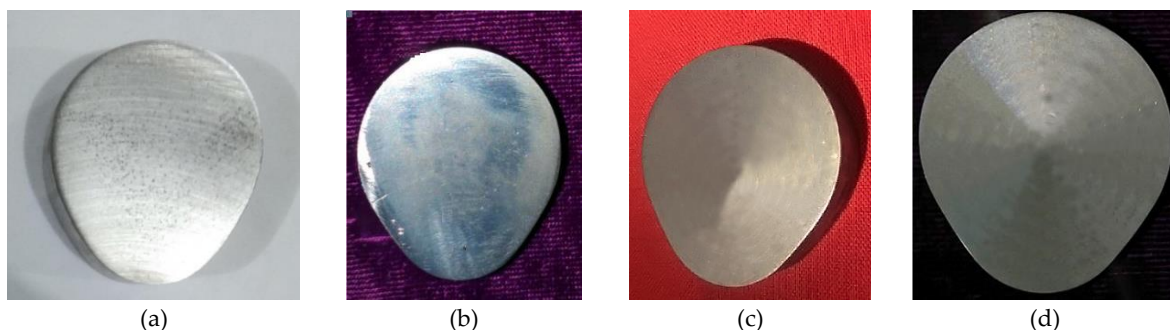


Figure 2. Camshaft manufacturing results (a) Specimen 1, (b) Specimen 2, (c) Specimen 3, and (d) Specimen 4

Table 2. Parameters of Testing Specimens

Specimens	Induction Hardening		Tempering	
	Heating time (s) (t1)	Output Current (A)	Holding time (s) (t2)	Temperature (°C) (T2)
1	15	747	15	150
2	20	747	20	150
3	15	985	15	250
4	20	985	-	-

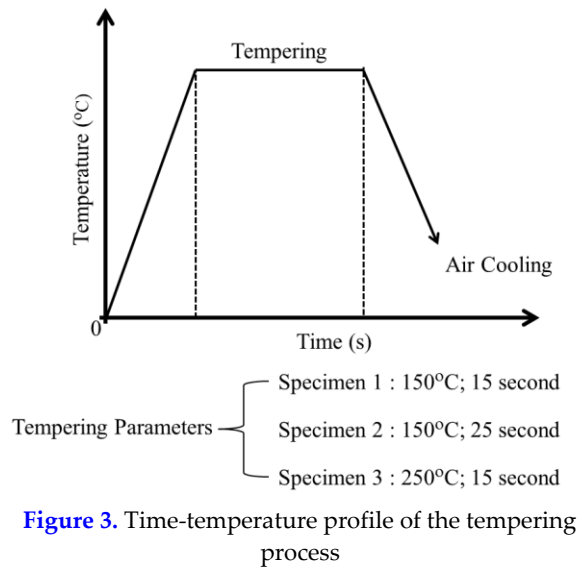


Figure 3. Time-temperature profile of the tempering process



Figure 4. Induction hardening failure in specimen 4

(side A), left (side B), and bottom (side C) of the camshaft specimen with 5 test points each.

Hardness testing on sides A, B, and C is intended to determine the distribution of hardness on the contour of the camshaft lobe. Sides A, B, and C show the heel, ram gap, and nose in the camshaft lobe. In this study, the first point of the hardness test was performed at a distance of 2 mm from the edge of the sample, and the next point was continued at a distance of 3 mm from each point. Details of hardness testing on sides A, B, and C of the camshaft specimen are shown in **Figure 5**. **Figure 6** shows the indentation marks on sides A, B, and C of the camshaft specimen after the hardness test.

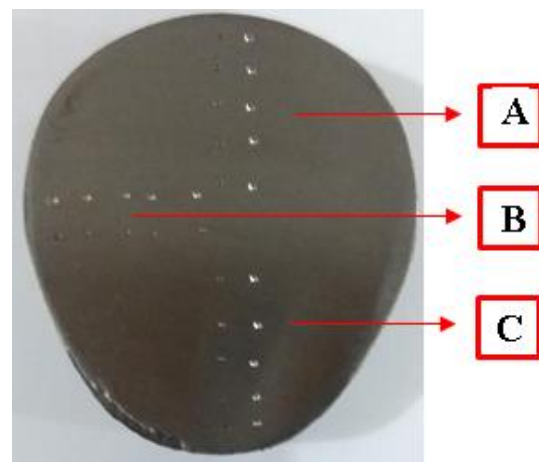


Figure 6. Indentation marks after hardness test

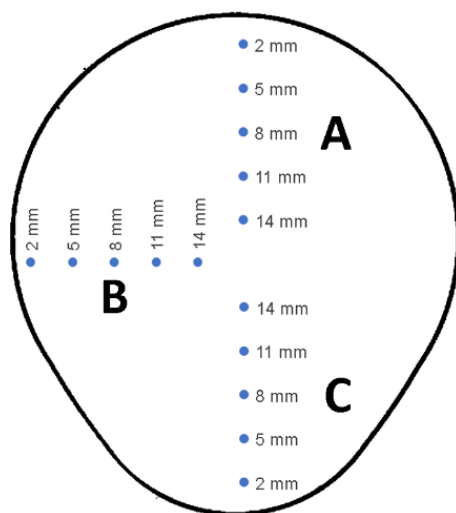


Figure 5. Indentation distribution in the camshaft hardness test

Rockwell testing in this study used a load of 150 kgf with a loading time of 30 seconds following the standard of ASTM E18-11 [7], [19]. The hardness testing was carried out on the top

In this study, the wear tests were carried out using the Ogoshi abrasion wear test machine (OAT-U type). The results of this test are used to determine the effect of induction hardening and tempering on specific wear on the camshaft material made of HQ 705 steel. In this test, the specimens carried out abrasive wear using a rolling steel disc. Specific wear value ($\text{mm}^3/\text{Kg}\cdot\text{mm}$) can be determined using the following Eq. 1 [20], [21].

$$W_s = \frac{B \cdot b^3}{8 \cdot r \cdot F \cdot L} \quad (1)$$

Where:

B = width of the disc (mm), 3 mm

r = disc radius (mm), 14 mm

F = wear load (kg), 6.3 Kg

L = length of disc track during rotation (mm), 200000 mm

b = width of scratch marks on specimen surface (mm)

3. Results and Discussion

The hardness test results after the induction hardening and tempering process on sides A, B, and C are shown in Figure 7 and Figure 8. Based on Figure 7, the maximum hardness achieved in this study is 50 HRC on specimen 3. In specimens 1 and 3, hardening induction was carried out with the same heating time of 15 seconds, but the output current used was different by 747 A and 985 A. The hardness test results show that specimen 3 has a greater hardness than specimen 1 at all test points. In specimen 1, the increase in hardness only occurred in the case/ surface and decreased as it approached the core. The higher the output current used in the induction hardening process with the same heating time, the greater the heat generated. This will result in heating propagation in the austenite phase. After a rapid cooling process, the austenite phase changes to a tough and brittle martensite phase [7], [22]–[24].

In other words, the higher the current used in the induction hardening process, the higher the hardness and hardness distribution across the cross-sectional area, as occurred in specimen 3.

The findings of this study are consistent with the literature [22], [25].

The hardness test results showed that specimen 2 had a greater hardness than specimen 1 at all test points. Induction hardening on specimens 1 and 2 was carried out with the same output current of 747 A, while the heating time was 15 and 20 seconds. An increase in heating time with the same current output in the induction hardening process will increase the hardness value [24], [26]. The longer heating time in the induction hardening process results in greater heat propagation in the austenite phase. With a fast cooling process, the austenite phase will turn into a hard and brittle martensitic material [7], [22]–[24]. As a result, the hardness and hardness distribution across the cross-sectional area of specimen 2 is greater than that of specimen 1.

Induction hardening performed on specimens 1 and 2 resulted in an increase in hardness which only occurred in the case/surface and decreased as it approached the core. The induction hardening on specimens 1 and 2 was effective, as evidenced by the decrease in hardness with increasing distance from the surface. Induction produces a high surface hardness that can withstand

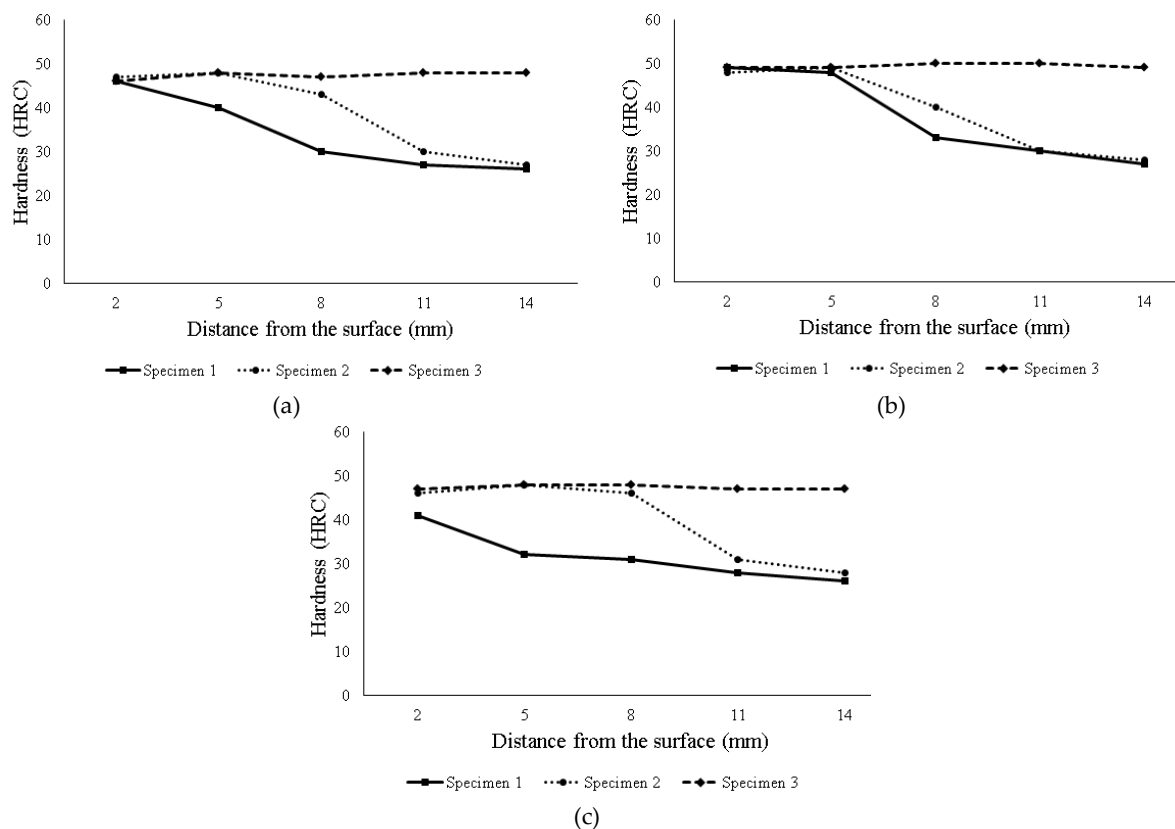


Figure 7. Hardness profile obtained after induction hardening on (a) side A, (b) side B, and (c) side C

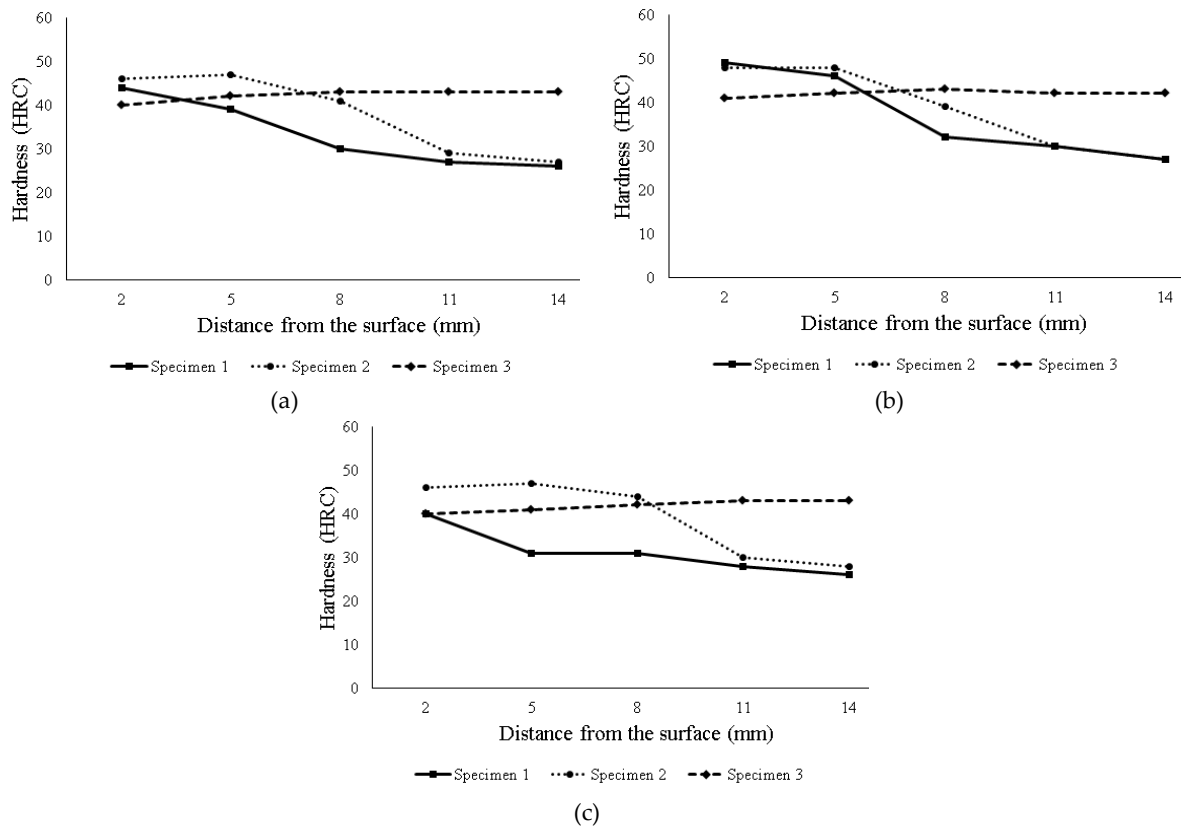


Figure 8. Hardness profile obtained after tempering on (a) side A, (b) side B, and (c) side C

extremely high loads. The development of a soft-core surrounded by an extremely tough outer layer increases fatigue strength [14]. Whereas in specimen 3, the induction hardening process resulted in changes in the hardness value in all parts of the specimen (case/surface, transition area, and core area) which is indicated by nearly the same hardness value at each measurement distance from the surface.

In general, induction hardening is used to selectively harden an area or part of a part without affecting the overall properties [27]. In this study, the maximum induction hardening and tempering parameters were obtained in Specimen 1. After induction hardening and tempering were carried out, the increase in the hardness of specimen 1 only occurred on the surface/ case. The closer to the core, the smaller the hardness, and there was not much difference from the hardness of the material before induction hardening, and tempering is carried out, 25 HRC as shown in Figure 8. Meanwhile, the hardness in the core area of specimens 2 and 3 was greater than the hardness of the raw materials.

Figure 9 shows the hardness of the material after induction hardening and induction hardening with tempering treatment. The

tempering process on specimens 1 and 3 is carried out at 150 °C and 250 °C, respectively, for 15 seconds. The highest decrease in hardness occurred at 250 °C, with a decrease in hardness reaching 7 HRC. While at a temperature of 150 °C, there was a decrease in hardness of 2 HRC. The greater the tempering temperature at the same heating time will result in a more significant decrease in hardness. The higher the tempering temperature, the greater the energy absorbed. Consequently, the tempered samples provide a good combination of mechanical properties because these processes reduce brittleness by increasing flexibility and toughness. Simultaneously, the hardness decreases with increasing tempering temperature [13], [28]–[30]. The tempering process in specimens 1 and 2 was carried out with tempering times of 15 seconds and 20 seconds with a temperature of 150 °C. The longer the tempering time, the amount of martensite phase decreases, and the austenite phase increases.

The austenite phase is softer than martensite, so the hardness decreases [31]. In this study, an increase in tempering time will reduce the value of hardness by 1-8 HRC. When a camshaft specimen is tempered, the martensite phase is

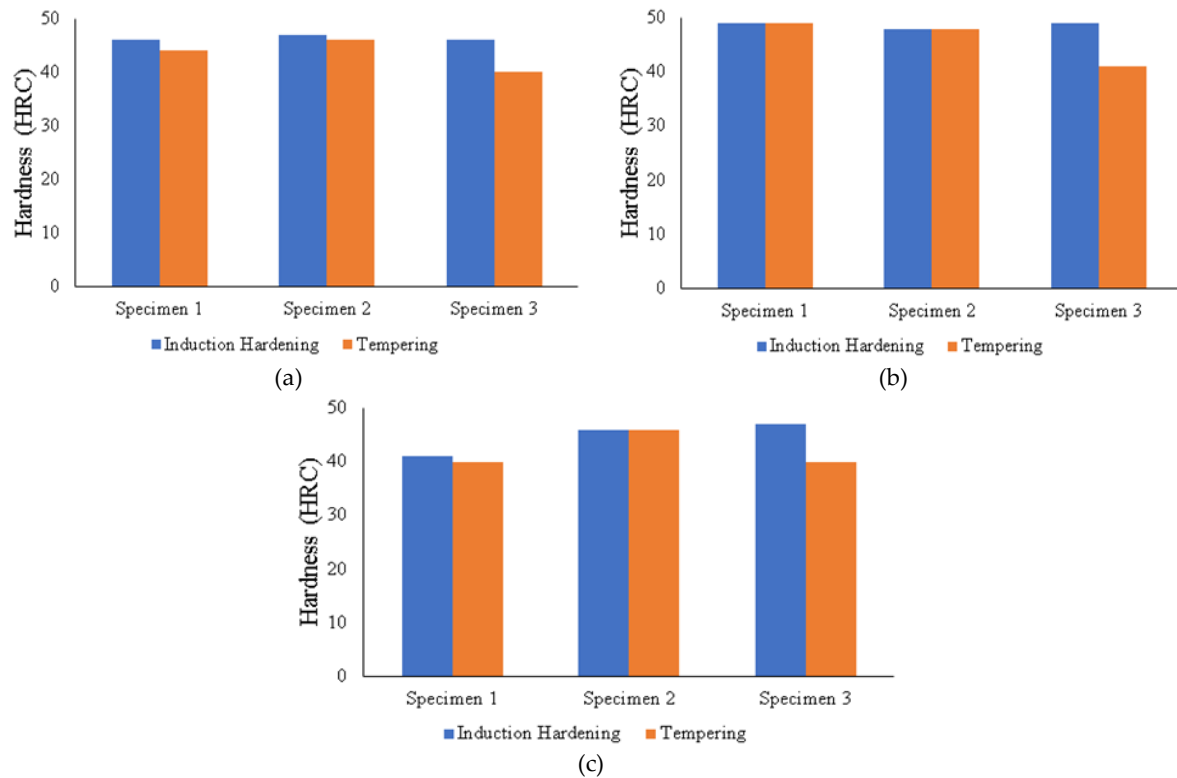


Figure 9. Differences in maximum hardness value after induction hardening and tempering on (a) side A, (b) side B, and (c) side C

transformed into various other phases. The carbon atoms in the martensite move out of the spaces between the iron atoms during the tempering process, forming iron carbide particles. As carbon atoms move out from between the iron atoms in martensite, the strain within the material is relieved. The ductility of the steel improves as a result, and the hardness of the steel decreases. The amount of hardness reduction after tempering is determined by the tempering time and temperature.

Figure 10 shows the macro photographs of the specimens after induction hardening and tempering. In specimens 1 and 2 (**Figure 10a** and

Figure 10b), the hardened zone produced is visible. Meanwhile, in specimen 3 (**Figure 10c**), hardened occurs in all parts of the specimen. The hardening layer in the hardened sample is indicated by the darker periphery of the specimen, as shown in **Figure 10**. The hardening layer on specimen 1 is thinner than specimens 2 and 3. The hardening layer is still clearly visible in specimen 2 with a dark color that is more dominant than the gray color (core).

In specimen 3, the specimen's surface is entirely dark. This demonstrates that the hardening layer in specimen 3 occurs throughout the specimen. The thicker the hardening layer, the

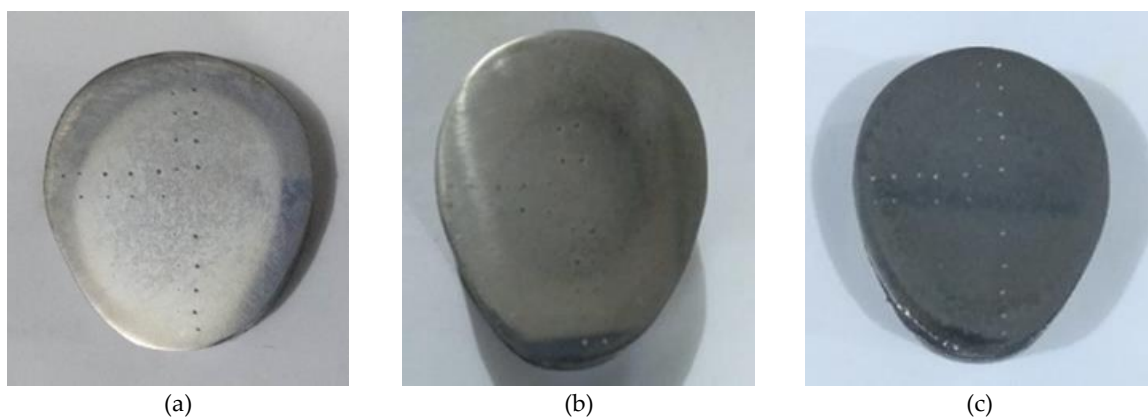


Figure 10. Hardness profile of (a) specimen 1, (b) specimen 2, and (c) specimen 3.

greater the distribution of hardness across the cross-sectional area of the sample. The presence of a thin and hard layer on specimen 1 provides excellent resistance to contact loads with the valve train.

In the macro photographs, it is clear that specimen 4 melted during the induction hardening process due to prolonged heating time using a large output current (Figure 4). The temperature imposed on the specimen 4 increases and reaches the melting point when a large output current and a long heating duration are combined in the induction heating process. As a result of using this parameter, Specimen 4 melted. The best results of this study were found in specimen 1 because the hardening only occurred in the case/surface. However, this study's uneven distribution of hardness and the resulting hardness profile did not resemble camshaft geometry.

The results of the microstructure test with 600x magnification of this study can be seen in Figure 11. Figure 11a shows that the microstructure of the

HQ 705 specimen (raw material) is tempered martensite (TM). Martensite has a body-centered tetragonal (BCT) crystal structure and is a very hard metastable structure. The microstructure of pure martensite is needle-like, but as it is tempered, the microstructure changes to a bushy type and carbides begin to precipitate on it. Tempering is a three-step process in which unstable martensite decomposes into ferrite and unstable carbides, and then into stable cementite, resulting in various stages of tempered martensite. Tempered martensite consists of the stable ferrite and cementite phases.

Its microstructure is similar to the microstructure of spheroidite but in this case tempered martensite contains extremely small and uniformly dispersed cementite particles embedded within a continuous ferrite matrix. Tempered martensite may be nearly as hard and strong as martensite but with substantially enhanced ductility and toughness [13], [28]–[30]. The annealing process is carried out on HQ 705 to relieve the martensitic phase. After the annealing

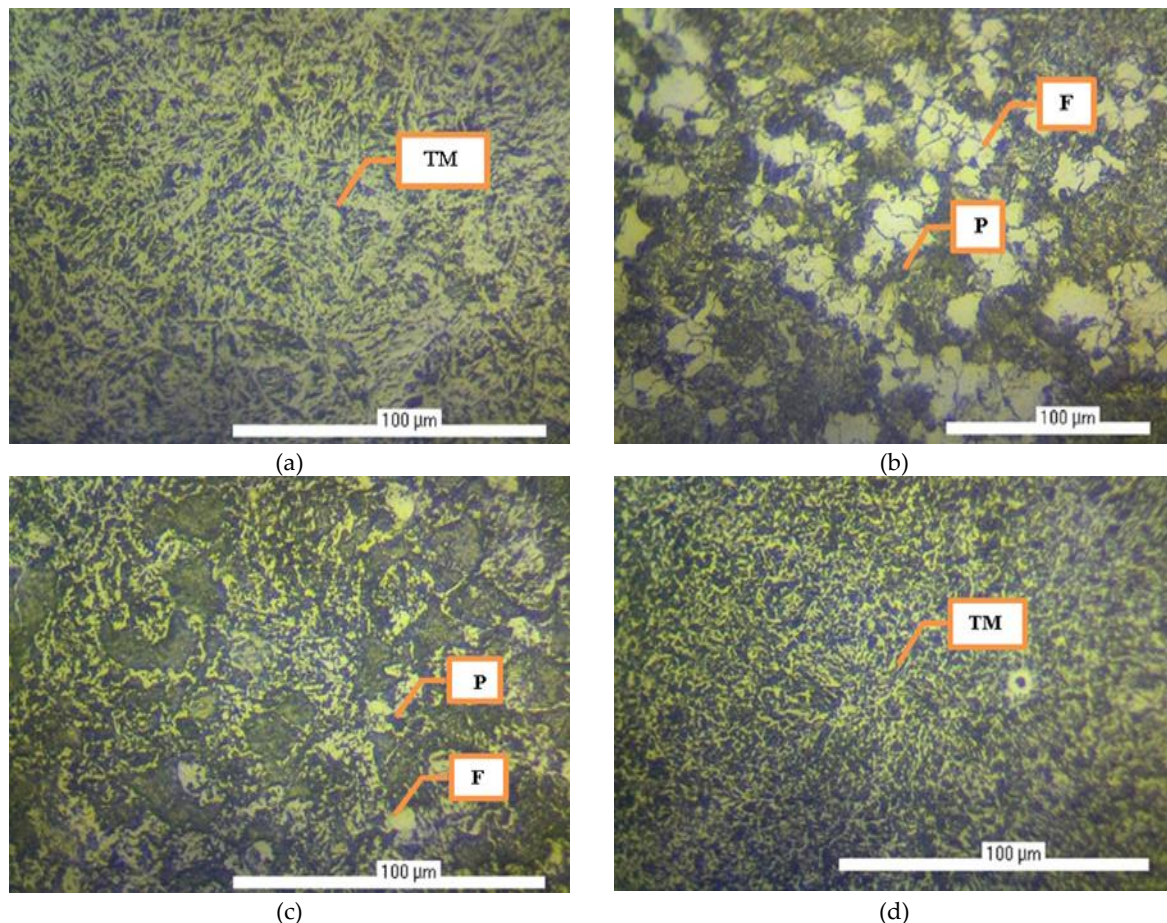


Figure 11. Microstructure evolution of (a) raw material HQ 705 (b) annealed HQ 705 (c) the core of specimen 1 (d), the surface of specimen 1

process, the tempered martensite changes phase to ferrite (F) and pearlite (P) which is shown in [Figure 11b](#).

[Figure 11b](#) shows that the microstructures that exist are ferrite and pearlite. The structure of ferrite is light in color, whereas the structure of pearlite is darker in color; both have large and coarse grain sizes. Pearlite has a hard structure due to the carbon content of the phase, whereas ferrite is soft and ductile. The findings of this study are consistent with the literature [32], [33].

This evidence shows that the annealing process successfully eliminated the martensite phase and reduced hardness by 7 HRC from the initial hardness. On the other hand, the results of microstructure testing on the core of specimen 1 after the induction hardening and tempering treatment did not change much, as shown in [Figure 11c](#). Thus, it made the induction process of hardening and tempering not significantly affect the hardness value in the core of specimen 1. Meanwhile, changes in the microstructure of the surface after the induction hardening and tempering of specimen 1 treatment are shown in [Figure 11d](#).

The microstructure of the surface of specimen 1 changed from the ferrite (F) and pearlite (P) phase to the tempered martensite (TM) phase. Optical microscopy observations showed that the center (core) of specimen 1 had a microstructure made from a mixture of ferrite and pearlite. Specimen 1 has a hard surface with a tempered martensite microstructure. The presence of this hardening layer was confirmed by microhardness testing. This is consistent with the hardness value of specimen 1 on the case/ surface, which has increased by 20-24 HRC. Meanwhile, the core hardness of specimen 1 is not significantly different from the raw material. The raw

material's surface hardness is 25 HRC (annealed). The core hardness of specimen 1 after induction hardening and tempering was 25–27 HRC (measurements at a distance from the surface were 11 and 14 mm on sides A, B, and C).

Wear tests were carried out on annealed HQ 705 and specimen 1. The width of the scratch mark on the specimen surface (b) is the average value of some measurements (i.e. b1, b2, b3, b4, b5, b6) as measured by a microscope observation as shown in [Figure 12](#). From the microscope observation results, b on the annealed HQ 705 and specimen 1 were 1.29 mm and 1.05 mm.

Specific wear value ($\text{mm}^3/\text{Kg}\cdot\text{mm}$) on the annealed HQ 705 and specimen 1 were $4.51 \times 10^{-8} \text{ mm}^3/\text{Kg}\cdot\text{mm}$ and $2.46 \times 10^{-8} \text{ mm}^3/\text{Kg}\cdot\text{mm}$, respectively. The raw material of HQ 705 steel (with annealing treatment) has a hardness of 25 HRC, and this hardness rises to 44 HRC after induction hardening and tempering treated (specimen 1). The induction hardening and tempering will be increasing hardness and decreasing specific wear. The higher hardness of the specimen leads to a decrease in wear rate [34]–[37].

4. Conclusion

The increase of hardness on the surface of the camshaft material made from HQ 705 steel using the induction hardening method with tempering has been investigated. The higher the output current and heating time used in the induction hardening process, the greater the heat generated. This will result in heating propagation in the austenite phase. After a rapid cooling process, the austenite phase changes to a tough and brittle martensite phase. However, if the output current used is too large, the heat applied to the material

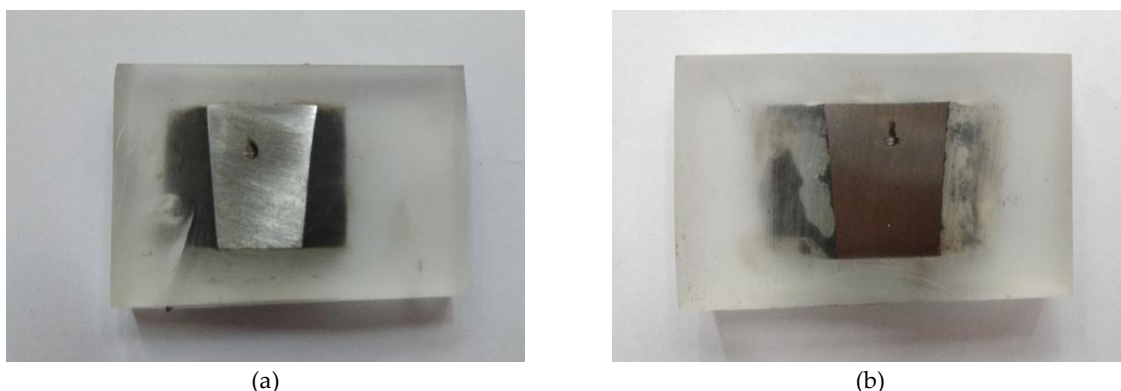


Figure 12. The scratch mark width of the disc on the surface (a) annealed HQ 705, (b) specimen 1

is too high, so that during rapid cooling there is a phase change from austenite to martensite in all parts of the material. This results in an increase in the hardness of all parts as happened in specimen 3. In addition, if the output current used is too large with a heating duration that is too long it can cause the heat applied to the material to reach the melting point and cause the material to melt as happened in specimen 4. The tempering process performed in this study has been shown to reduce the hardness of all samples. The amount of hardness reduction after tempering is determined by the tempering time and temperature.

Induction hardening performed with an output current of 747 A for 15 seconds with tempering at a temperature of 150 °C for 15 seconds on specimen 1 gave the best surface hardening result. The increase in hardness in specimen 1 only occurred in the case/ surface and decreased as it approached the core. This happens because the tempered martensite phase is only found in the case/ surface of specimen 1. While the core of specimen 1 has the same microstructure as annealed HQ 705 (ferrite and pearlite). Hardness on the case/ surface of specimen 1 is 44 HRC, with a hardness on a core is 26 HRC. The increase in hardness on the case/ surface of specimen 1 resulted in a better wear resistance than annealed HQ 705. This is because the induction hardening and tempering processes carried out on specimen 1 resulted in a 46% decrease in specific wear ($2.46 \times 10^{-8} \text{ mm}^3/\text{Kg.mm}$).

However, the surface hardness of the camshaft made of HQ 705 steel produced in this study does not meet the minimum hardness requirement for the camshaft material, which is 45 HRC. Furthermore, this study resulted in an uneven hardness distribution and a hardness profile that does not resemble the camshaft geometry. This is due to the fact that the coil used in this study is circular and does not resemble the shape of the camshaft. Furthermore, because the camshaft has contours with different geometries, the static method causes heat to be applied to the material unevenly.

Acknowledgement

The authors would like to express their gratitude to the Diponegoro University for the non-APBN research funding in Riset Pengembangan dan Penerapan (RPP) in 2018-

2019. Authors also would like to thank to Agency for the Assessment and Application of Technology (BPPT) for providing the camshaft specimens.

Author's Declaration

Authors' contributions and responsibilities

The authors made substantial contributions to the conception and design of the study. The authors took responsibility for data analysis, interpretation and discussion of results. The authors read and approved the final manuscript.

Funding

Riset Pengembangan dan Penerapan (RPP) in 2018-2019, Diponegoro University.

Availability of data and materials

All data are available from the authors.

Competing interests

The authors declare no competing interest.

Additional information

No additional information from the authors.

References

- [1] J. A. Vélez Godiño, M. T. García, F. J. J. E. Aguilar, and D. P. Guerrero, "Failure analysis of an overhead valve train system in urban buses," *Engineering Failure Analysis*, vol. 96, no. November 2018, pp. 455–467, 2019, doi: 10.1016/j.engfailanal.2018.11.003.
- [2] H. Zhou, D. Zhao, Y. Liu, and G. Li, "Influence of Induction Hardening Process on Camshafts' Residual Stresses," *Arabian Journal for Science and Engineering*, vol. 45, no. 11, pp. 9651–9659, 2020, doi: 10.1007/s13369-020-04878-9.
- [3] X. lei Xu, Z. wei Yu, and S. mei Mao, "Effect of extra-large compound calcium-aluminosilicate inclusions on cracking of camshafts," *Engineering Failure Analysis*, vol. 110, no. June 2019, p. 104408, 2020, doi: 10.1016/j.engfailanal.2020.104408.
- [4] G. Doyon, V. Rudnev, J. Maher, R. Minnick, and G. Desmier, "Elimination of straightening operation in induction hardening of automotive camshafts," *International Journal of Microstructure and Materials Properties*, vol. 11, no. 1–2, pp. 119–133, 2016, doi: 10.1504/IJMMP.2016.078032.
- [5] J. Choi and S. Lee, "High-frequency heat treatment of aisi 1045 specimens and current calculations of the induction heating coil

- using metal phase transformation simulations," *Metals*, vol. 10, no. 11, pp. 1–11, 2020, doi: 10.3390/met10111484.
- [6] B. Karaca and M. Şimşir, "The effects of austempering and induction hardening on the wear properties of camshaft made of ductile cast iron," *Acta Physica Polonica A*, vol. 131, no. 3, pp. 448–452, 2017, doi: 10.12693/APhysPolA.131.448.
- [7] N. F. D. S. Guterres, Rusnaldy, and A. Widodo, "The Effect of Temperature in Induction Surface Hardening on the Distortion of Gear," *IOP Conference Series: Materials Science and Engineering*, vol. 202, no. 1, 2017, doi: 10.1088/1757-899X/202/1/012092.
- [8] M. Leitner, F. Grün, Z. Tuncali, and W. Chen, "Fatigue and Fracture Behavior of Induction-Hardened and Superimposed Mechanically Post-treated Steel Surface Layers," *Journal of Materials Engineering and Performance*, vol. 27, no. 9, pp. 4881–4892, 2018, doi: 10.1007/s11665-018-3543-z.
- [9] H. Yamagata, "The camshaft," in *The Science and Technology of Materials in Automotive Engines*, H. B. T.-T. S. and T. of M. in A. E. Yamagata, Ed. Woodhead Publishing, 2005, pp. 110–131.
- [10] R. Singh, "6 - Classification of steels," in *Applied Welding Engineering (Third Edition) Processes, Codes, and Standards*, R. B. T.-A. W. E. (Third E. Singh, Ed. Butterworth-Heinemann, 2020, pp. 53–60.
- [11] V. Malau and L. Arifudin, "Vickers Microhardness Dependence Load and Determining of Tensile Strength of HQ 705 Steel from Microhardness Curves Vickers Microhardness Dependence Load and Determining of Tensile Strength of HQ 705 Steel from Microhardness Curves," *Applied Mechanics and Materials*, no. June, 2016, doi: 10.4028/www.scientific.net/AMM.842.43.
- [12] J. Zhao, "22 - The use of ceramic matrix composites for metal cutting applications," in *Advances in Ceramic Matrix Composites*, I. M. B. T.-A. in C. M. C. Low, Ed. Woodhead Publishing, 2014, pp. 537–569.
- [13] N. M. Ismail, N. A. A. Khatif, M. A. K. A. Kecik, and M. A. H. Shaharudin, "The effect of heat treatment on the hardness and impact properties of medium carbon steel," *IOP Conference Series: Materials Science and Engineering*, vol. 114, no. 1, pp. 0–9, 2016, doi: 10.1088/1757-899X/114/1/012108.
- [14] R. Ismail, D. I. Prasetyo, M. Tauviqirrahman, E. Yohana, and A. P. Bayuseno, "Induction hardening of carbon steel material: The effect of specimen diameter," *Advanced Materials Research*, vol. 911, pp. 210–214, 2014, doi: 10.4028/www.scientific.net/AMR.911.210.
- [15] J. Hájek, D. Rot, and J. Jiřinec, "Distortion in induction-hardened cylindrical part," *Defect and Diffusion Forum*, vol. 395 DDF, no. August, pp. 30–44, 2019, doi: 10.4028/www.scientific.net/DDF.395.30.
- [16] H. T. Zhang, X. Y. Dai, J. C. Feng, and L. L. Hu, "Preliminary investigation on real-time induction heating-assisted underwater wet welding," *Welding Journal*, vol. 94, no. 1, pp. 8s-15s, 2015.
- [17] L. Rothleutner, C. Van Tyne, and R. Goldstein, "Influence of vanadium microalloying on the microstructure of induction hardened 1045 steel shafts," *ASM International - 29th Heat Treating Society Conference, HEAT TREAT 2017*, vol. 2017-October, pp. 201–210, 2017.
- [18] C. Lorenzo-Martin and O. O. Ajayi, "Rapid surface hardening and enhanced tribological performance of 4140 steel by friction stir processing," *Wear*, vol. 332–333, pp. 962–970, 2015, doi: <https://doi.org/10.1016/j.wear.2015.01.052>.
- [19] ASTM Standard E18 - 11, *Standard Test Methods for Rockwell Hardness of Metallic Materials*. ASTM International, 2012.
- [20] C. Pramono, X. Salahudin, I. Taufik, A. Bagaskara, and D. M. Irawan, "Study of mechanical properties of composite strengthened mango seed powder (mangifera indica cultivar manalagi), brass, and magnesium oxide for brake pads material," *Journal of Physics: Conference Series*, vol. 1517, no. 1, 2020, doi: 10.1088/1742-6596/1517/1/012012.
- [21] N. Wahyuni, R. Nur, I. Renreng, and M. Adnan, "Effect of adding SiC on resistance wear and hardness through stir casting of aluminum matrix composites," *AIP Conference Proceedings*, vol. 2114, no. 050020, p. 30019, 2019, doi: 10.1063/1.5112464.
- [22] A. Kohli and H. Singh, "Optimization of processing parameters in induction

- hardening using response surface methodology," *Sadhana - Academy Proceedings in Engineering Sciences*, vol. 36, no. 2, pp. 141–152, 2011, doi: 10.1007/s12046-011-0020-x.
- [23] H. Hammi, A. El Ouafi, and N. Barka, "Study of frequency effects on hardness profile of spline shaft heat-treated by induction," *Journal of Materials Science and Chemical Engineering*, vol. 4, no. 3, pp. 1–9, 2016, doi: 10.4236/msce.2016.43001.
- [24] S. P. Metage and J. S. Sidhu, "Optimization of Process Parameters in Induction Hardening of 41Cr4 Steel by Response Surface Methodology," *International Journal of Mechanical Engineering Research*, vol. 7, no. 2, pp. 83–97, 2017.
- [25] H. Purwanto, M. Dzulfikar, and M. Tauviqirrahman, "The Effect of Austenization Temperature in Surface Hardening Process on Steel Plate as Ballistic Plate," *Journal of Physics: Conference Series*, vol. 1908, pp. 1–8, 2021, doi: 10.1088/1742-6596/1908/1/012030.
- [26] M. Onan, K. Baynal, and & H. Ünal, "Determining the influence of process parameters on the induction hardening of AISI 1040 steel by an experimental design method," *Indian Journal of Engineering & Materials Sciences*, vol. 22, pp. 513–520, 2015.
- [27] V. Rudnev, D. Loveless, and R. L. Cook, "Theoretical Background," in *Handbook of Induction Heating*, 2nd ed., CRC press taylor & francis group, 2017.
- [28] O. Haiko *et al.*, "The effect of tempering on the microstructure and mechanical properties of a novel 0.4C press-hardening steel," *Applied Sciences (Switzerland)*, vol. 9, no. 20, pp. 1–16, 2019, doi: 10.3390/app9204231.
- [29] C. Zhang *et al.*, "Effect of tempering temperature on impact wear behavior of 30cr3mo2wni hot-working die steel," *Frontiers in Materials*, vol. 6, no. July, pp. 1–8, 2019, doi: 10.3389/fmats.2019.00149.
- [30] S. Herbirowo, B. Adjiantoro, T. B. Romijarso, and A. W. Pramono, "The effect of tempering treatment on mechanical properties and microstructure for armored lateritic steel," *AIP Conference Proceedings*, vol. 1964, no. May, 2018, doi: 10.1063/1.5038325.
- [31] S. Sen R. Kumar, R. K. Behera, "Effect of Tempering Temperature and Time on Strength and Hardness of Ductile Cast Iron," *IOP Conf. Series: Materials Science and Engineering*, vol. 75, no. 2015, pp. 1–9, 2015, doi: 10.1088/1757-899X/75/1/012015.
- [32] S. D. Martín, de T. Cock, A. García-Junceda, F. G. Caballero, C. Capdevila, and C. G. de Andrés, "Effect of heating rate on reaustenitisation of low carbon niobium microalloyed steel," *Materials Science and Technology*, vol. 24, no. 3, pp. 266–272, Mar. 2008, doi: 10.1179/174328408X265640.
- [33] M. Jafarzadegan, A. Abdollah-zadeh, A. H. Feng, T. Saeid, J. Shen, and H. Assadi, "Microstructure and Mechanical Properties of a Dissimilar Friction Stir Weld between Austenitic Stainless Steel and Low Carbon Steel," *Journal of Materials Science and Technology*, vol. 29, no. 4, pp. 367–372, 2013, doi: 10.1016/j.jmst.2013.02.008.
- [34] D. F. Fitriyana *et al.*, "The Effect of Post-Heat Treatment on The Mechanical Properties of FeCrBMnSi Coatings Prepared by Twin Wire Arc Spraying (TWAS) Method on Pump Impeller From 304 Stainless Steel," *Journal of Advanced Research in Fluid Mechanics and Thermal Sciences*, vol. 2, no. 2, pp. 138–147, 2022.
- [35] D. F. Fitriyana *et al.*, "The Effect of Compressed Air Pressure and Stand-off Distance on the Twin Wire Arc Spray (TWAS) Coating for Pump Impeller from AISI 304 Stainless Steel," *Springer Proceedings in Physics*, vol. 242, pp. 119–130, 2020, doi: 10.1007/978-981-15-2294-9_11.
- [36] R. Zhang, J. Li, D. Yan, and Y. Zhao, "Mechanical Properties of WC-8Co Wear-Resistant Coating on Pump Impellers Surface by Electro- Spark," *Rare Metal Materials and Engineering*, vol. 44, no. 7, pp. 1587–1590, Jul. 2015, doi: 10.1016/S1875-5372(15)30097-7.
- [37] V. Malau and W. I. Fauzi, "Effects of Heat Treatments on Mechanical Properties, Specific Wear and Corrosion Rate of HQ 809 Steel for Machinery Components Application," *Proceedings - 2018 4th International Conference on Science and Technology, ICST 2018*, Nov. 2018, doi: 10.1109/ICSTC.2018.8528600.